Missing OH source in a suburban environment near Beijing : observed and modelled OH and HO_2 concentrations in summer 2006

Online supplementary materials

K. D. Lu[1,2], A. Hofzumahaus[2], F. Holland[2], B. Bohn[2], T. Brauers[2], H. Fuchs[2], R. Häseler[2], M. Hu[1], K. Kita[3], Y. Kondo[4], X. Li[1,2], S. R. Lou[2,5,*], A. Oebel[2,**], M. Shao[1], L. M. Zeng[1], A. Wahner[2], T. Zhu[1], Y H. Zhang[1], F. Rohrer[2]

[1]State Key Joint Laboratory of Environmental Simulation and Pollution Control, College of Environmental Sciences and Engineering, Peking university, Beijing, China
[2]Institut für Energie und Klimaforschung: Troposphäre, Jülich, Germany
[3]Faculty of Science, Lbaraki University, Lbaraki 310-8512, Japan
[4]University of Tokyo, Research Center for Advanced Science and Technology, Tokyo, Japan
[5]School of Environmental Science and Technology, Shanghai Jiaotong University, Shanghai 200240, China
∗ now at: Shanghai Academy Of Environmental Sciences, Shanghai, China
∗∗ now at: AIXTRON SE, Herzogenrath, Germany
To whom correspondence should be addressed. E-mail: f.rohrer@fz-juelich.de; yhzhang@pku.edu.cn.

This file includes:

1. HOx and k_{OH} measurement results in Sep 2006 (Fig. S1)
2. Averaged diurnal profiles of O_3, NO, NO_2, $j(NO_2)$, and VOC speciations for southerly wind days and that of Aug 20 (Fig. S2)
3. Intercomparsions of the modelled HOx concentrations between M0 and RACM-MIM-GK, and that between M5 (MCMv3.2) and MCMv3.1 (Fig. S3, Fig. S4)
4. Retrieved diurnal profiles of X and Y for M1 and M2 (Fig. S5)

1. HOx and k_{OH} measurement results in Sep 2006

We performed HOx and k_{OH} measurements during Sep 2006 as well as Aug 2006 (see Fig. S1). In general, similar levels of OH, HO_2 and k_{OH} values and diurnal variabilities were observed for both periods. In this study, the model analysis were limited to the time period in which high precision NO measurement was avaiable.

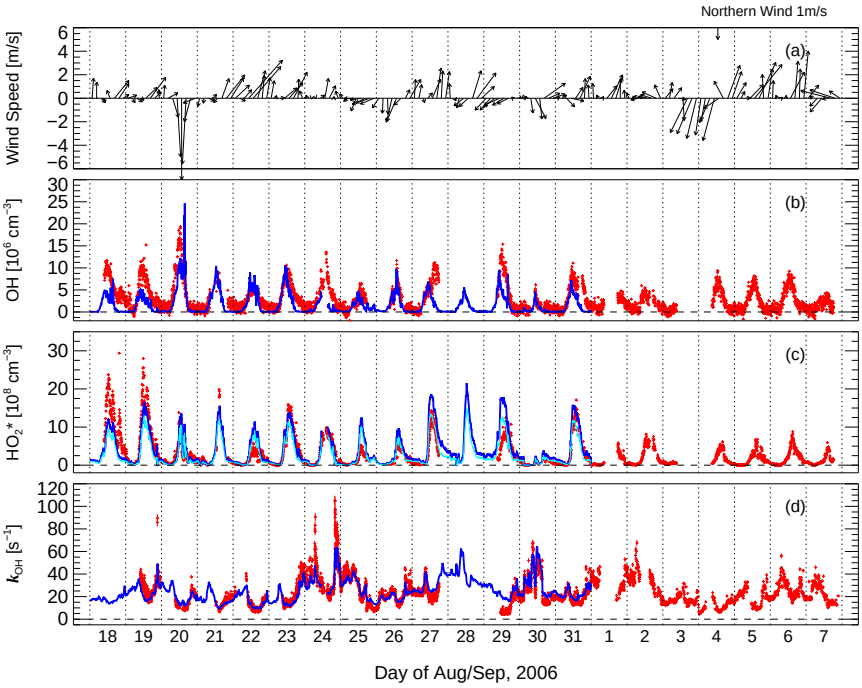

Figure S1. Full time series of the measured (red pluses) and M0 modeled (blue lines) OH, HO_2^* and k_{OH} at the Yufa site during CAREBeijing2006 campaign. Cyan line in panel (c) give the modeled HO_2. The model results are limited to the existence of the high precision NO data. The wind pattern is given as support information.

2. Averaged diurnal profiles of O_3, NO, NO_2, $j(NO_2)$, and VOC speciations for southerly wind days and that of Aug 20

In Fig. S2, we provide basic photochemical characteristics of the two periods, namely southerly wind days and Aug 20, in discussion of the main paper. For these two periods, similar $j(NO_2)$ and VOC speciation were observed whereas the major photochemical difference was characterized by the afternoon NOx concentrations.

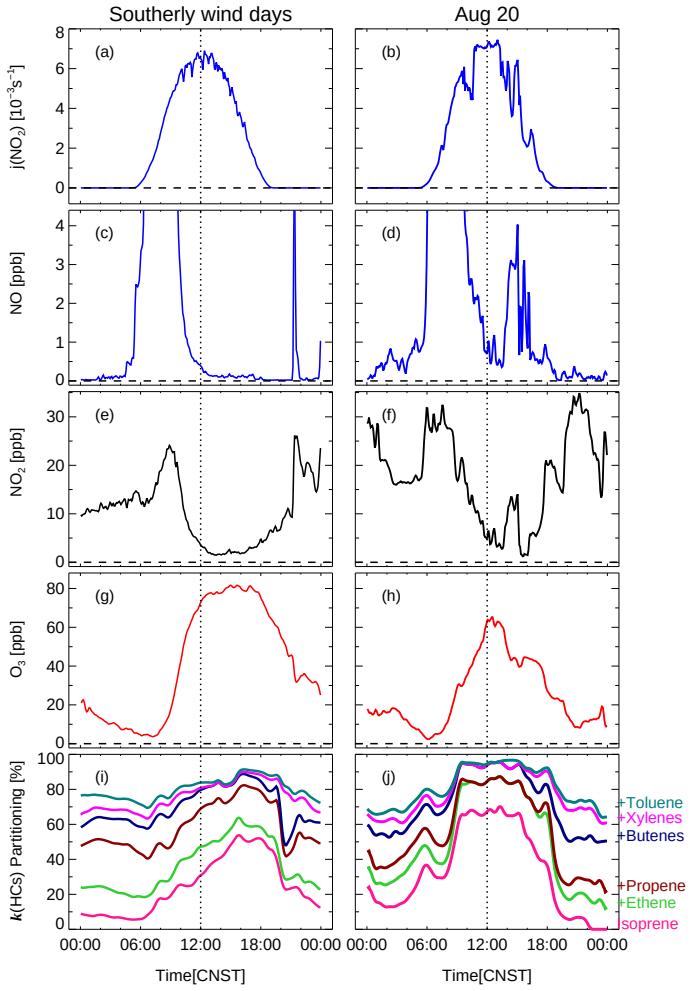

Figure S2. The averaged diurnal profiles of NO, NO_2, O_3, $j(NO_2)$ and the speciation of observed HC reactivities during southerly wind days and that of Aug 20. Butenes=1-Butene, *i*-Butene, *trans*-2-Butene, *cis*-2-Butene; Xylenes=*o*-,*m*-,*p*-Xylene.

3. Intercomparsions of the modelled HOx concentrations between M0 and model scenario with RACM-MIM-GK, and that between M5 (MCMv3.2) and model scenario with MCMv3.1

By including the R(C=O)R'O_2+HO_2→ OH chemistry proposed by Dillon and Crowley (2008); Jenkin et al. (2007) and the isoprene epoxide chemistry (Paulot et al., 2009) into RACM-MIM-GK, we defined the new base case model mechanism, namely M0. Similarly changes were done for MCMv3.1 and thus updated to be MCMv3.2 (see http://mcm.leeds.ac.uk/MCM/project.htt#New_3.2). As shown by Fig. S3 and Fig. S4, the impact on the modelled HOx concentrations by these two additions is small. For RACM-MIM-GK, the change is less than 1% for OH while about 2% for HO_2. For MCMv3.1, the change is about -2% for OH and 2% for HO_2. The reduction of modelled OH in MCMv3.2 is due to the reduced reaction rate constant of HO_2 + NO (-4%) which overcome the enhanced mechanistic OH recycling.

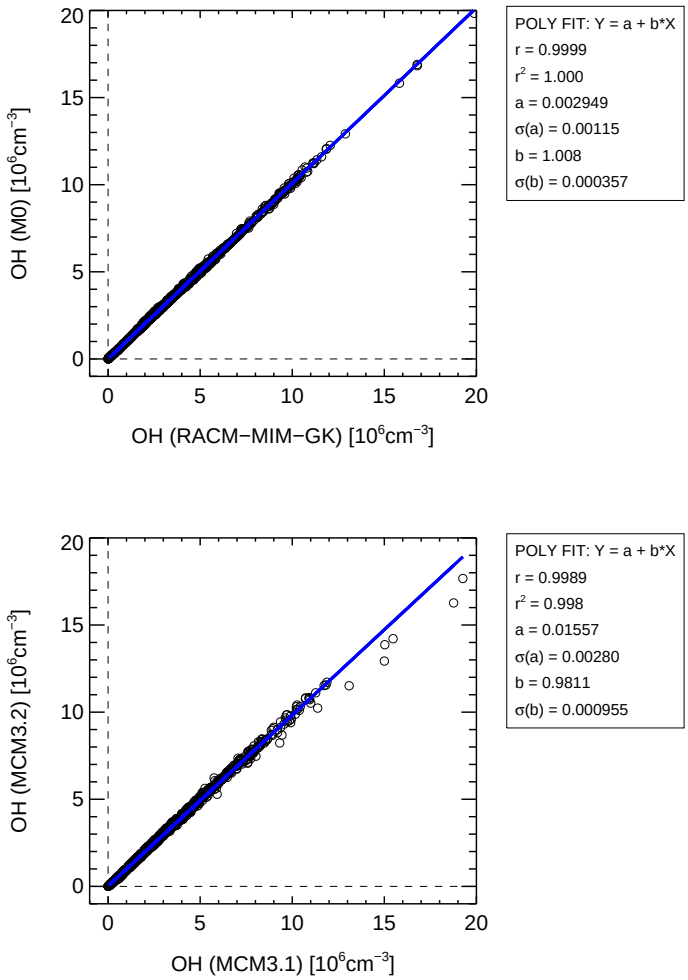

Figure S3. Regression analysis of the modelled OH concentrations between M0 and model scenario with RACM-MIM-GK, and those between M5 (MCMv3.2) and model scenario with MCMv3.1.

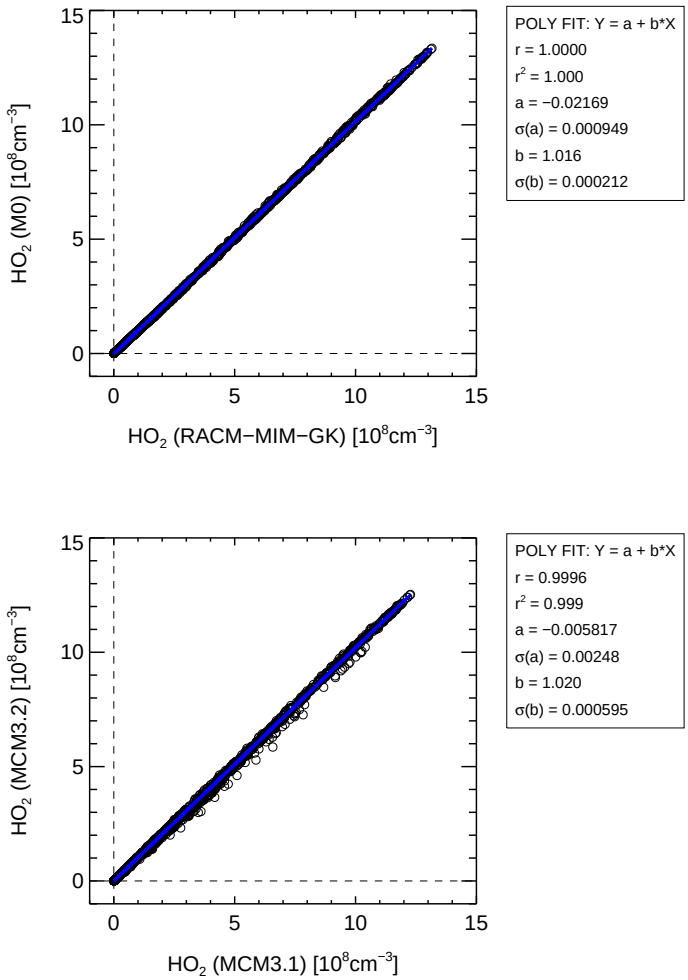

Figure S4. Regression analysis of the modelled HO_2 concentrations between M0 and model scenario with RACM-MIM-GK, and those between M5 (MCMv3.2) and model scenario with MCMv3.1.

4. Retrieved diurnal profiles of X and Y for M1 and M2

By taking observed OH concentrations as the target parameter, the numerically retrieved diurnal profiles of X and Y for M1 and M2, respectively, were shown as Fig. S5. The merit function in this retrieval is set to be

$$\chi^2 = \sum_{t=10:00}^{18:00} \left(\frac{\mathrm{OH}_{obs} - \mathrm{OH}_{mod}}{\sigma(\mathrm{OH}_{obs})}\right)^2 \tag{E1}$$

of which OH_{obs} denote the observed values, the OH_{mod} denote the modelled values, $\sigma(\mathrm{OH}_{obs})$ is taken as the measurement accuracy and the time window (10:00 – 18:00) for optimization is selected to match the daytime period when the model-measurement discrepancy of OH concentrations takes place (cf. Fig 8a in the main paper).

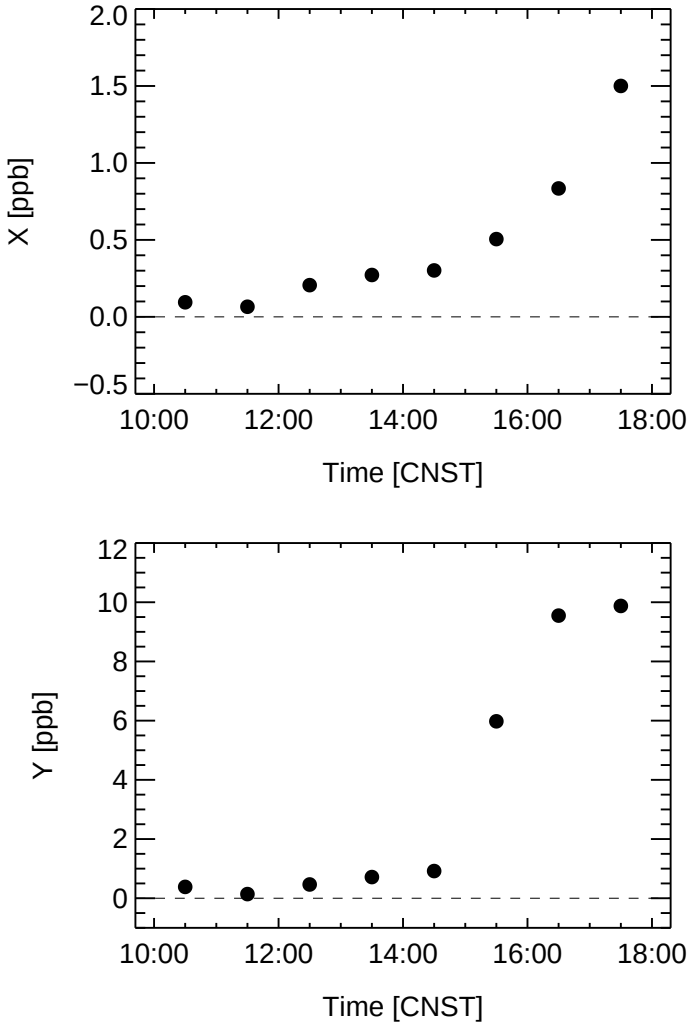

Figure S5. The retrieved diurnal profiles of X and Y for M1 and M2 during 10:00 – 18:00, respectively.

References

Dillon, T. J. and Crowley, J. N.: Direct detection of OH formation in the reactions of HO_2 with $CH_3C(O)O_2$ and other substituted peroxy radicals, Atmospheric Chemistry and Physics, 8, 4877–4889, doi:10.5194/acp-8-4877-2008, 2008.

Jenkin, M. E., Hurley, M. D., and Wallington, T. J.: Investigation of the radical product channel of the $CH_3C(O)O_2$+HO_2 reaction in the gas phase, Phys. Chem. Chem. Phys., 9, 3149–3162, 2007.

Paulot, F., Crounse, J. D., Kjaergaard, H. G., Kroll, J. H., Seinfeld, J. H., and Wennberg, P. O.: Isoprene photooxidation: new insights into the production of acids and organic nitrates, Atmos. Chem. Phys., 9, 1479–1501, doi:10.5194/acp-9-1479-2009, 2009.